# RELIABLE FIELD EMISSION ARRAY FOR X-RAY GENERATION WITH INORGANIC FILLER TREATED BY HIGH TEMPERATURE VACUUM ANNEALING

*B. Sun, Y. Wang, Q. Xing, G. Huang and G. Ding*
Shanghai Jiao Tong University, CHINA

## ABSTRACT

We design, model, optimize and fabricate cold electron cathodes that are specifically designed for X-ray sources. Micromachining patterning process, which enhanced edge effect, significantly improved its emission performance. High bonding strength was achieved by a preferred high temperature annealing process, which results in the improvement of field emission properties. To check its practical application, the fabricated emitter was vacuum sealed and tested in a conventional X-ray tube.

## INTRODUCTION

Carbon nanotubes (CNTs) exhibit excellent field emission characteristics due to their inherent small tip radius and high aspect ratio combined with robust chemical and mechanical stabilities.[1, 2] CNT field emission cold cathodes have been regarded as attractive electron sources in various applications such as field emission displays,[3] lighting devices,[4] x-ray tubes,[5] electron microscopy and microwave power amplifiers. Recently, much effort has been made to develop various methods for fabricating CNT field emitters. Direct growth,[6] electrophoresis,[7] and screen printing[8] have been recognized as three promising techniques for fabricating field emission cold cathode. Although many researchers have studied fabricating method of CNTs composited electrodes, there are still severe problems with their reliability and uniformity. The origin of these problems mainly lies in the weak interfacial bond strength between the substrate and CNTs.[9]

Up to now, CNT composited electrodes have mostly been synthesized by mixing CNT powders with organic vehicles.[10] Organic vehicles can easily soak CNTs and form a uniform bonding layer.[11] However, it is difficult for organic vehicles to be a matrix with high strength and chemical stability. Intense shrinkage in solidification process and low hardness of curing film result in weak adhesion of organic paste on CNTs.[12] Weak interfacial bond strength in CNTs/organic paste often induces escaping of CNTs from the binders at strong field. Water soluble inorganic binders present more adaptability for fabricating CNTs composited electrode due to its good soakage for CNTs, high hardness and chemical stability after high temperature treatment.[9, 13] Furthermore, a more demulcent shrinkage process is developed by dehydrating in inorganic binders compared with organic solvent volatizing. More uniform interfacial bond can be obtained in this process, which is beneficial to improve the interfacial bond strength. As a result, there have hardly been any CNT emitters using conventionally formulated organic pastes be commercialized.

In this paper, we choose an environmental water soluble inorganic material soluble glass (SG) as the binder, and prepare a carbon nanotubes (CNTs) based electro-conductive glass electrode (ECGE) with high bonding strength between solidified soluble glass (SG) and CNTs. The stress distribution of the cathode under electric field has been simulated by finite element method using COMSOL software. The interface between the CNTs and the cathode substrate near to the surface was proved a stress concentration area. So, the high bonding strength plays an important role for avoiding escaping of CNTs from the substrate. The changes that made by high temperature hardening process were studied by Thermo-gravimetric (TG) and Raman spectrum (RS). It showed that, a steady -Si-O- sheet formed around the CNTs during the high temperature hardening process, which enhanced the adhesion of CNTs to the sodium silicate. Less CNTs fragments were observed at the opposite anode of the hardened ECGE after field emission test through scanning electron microscope (SEM). The ECGE showed reliable operation at high emission current for effectively avoiding CNTs escaping phenomenon, making them applicable to novel field emission devices.

## EXPERIMENTAL

Multi-walled carbon nanotubes (MWNT) with an average diameter of 30-50 nm and varying lengths of 5-15 um (95% pure) were mixed with SG. The CNT paste was formulated using a mechanical ball milling machine (QM-QX04, Nanjing University Instrument Plant). The paste was uniformly deposited on a glass substrate. Then the glass substrate was placed in an oven under ambient atmosphere at 100 ℃ for 4 h. Polishing was then carried out to achieve a smooth field emission surface. Then the CNT field emitters were achieved by etching away a thin SG layer by hydrofluoric acid. The etching time and etching method were carefully controlled to ensure that the tips of the CNTs were exposed and the roots of the CNTs firmly embedded in the substrate. Finally, a high temperature hardening process was carried out in an oven under ambient atmosphere at 400 ℃ for 4 h.

The morphologies of the fabricated ECGE were characterized using a field emission scanning electron microscope (FESEM; Zeiss ultra 55, Germany). The Raman spectrum of the ECGE were obtained using a Raman microscope (Ram, Bruker Opties Senterra R200, US) with 10× and 100× objectives at a laser wavelength of 532 nm. Spectrum acquisitions were done with a power of 1mW with integration times of 10-60 s depending on the sample examined. Thermal analysis of the ECGE was carried out with a thermo-gravimetric analyzer (TGA Pyris 1, PerkinElmer, US) at atmospheric pressure with an air flow rate of 60 ml/min at a heating rate of 10 ℃/min from 30 to 600 ℃. Approximately 13.5 mg of sample was located in the Al crucible for the experiment.

The field emission characteristics of the ECGE were measured in a vacuum chamber with a parallel diode-type configuration at pressure of $1\times10^{-6}$ Torr as shown in Fig. 2 (b) (c). All of the samples were cut into the same size of 0.2cm×1 cm. A DC voltage was applied by a high-voltage power supply (HBGY HB-2502-100AC, China) across the cathode and the anode with a distance of 200μm. The current was measured and saved by a digit multimeter (Agilent 34401A, US). In order to protect high-voltage power supply from high-voltage arcing breakdown, a current-limiting resistor (3 MΩ) was used.

## RESULTS AND DISCUSSION

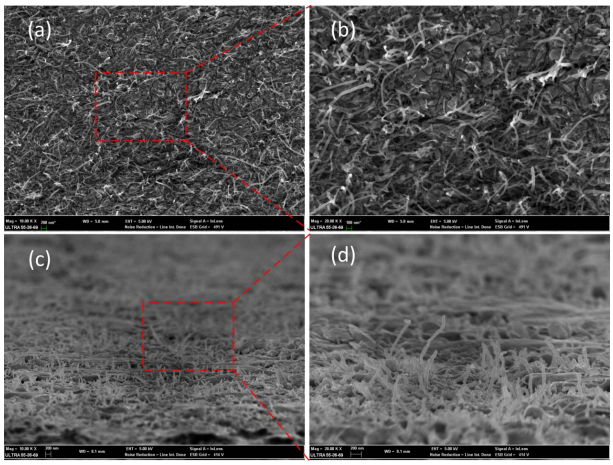


*Figure 1: SEM images of the fabricated ECGE. The images are from top (a) (b), and oblique (c) (d) directions.*

Figure 1 shows a series of SEM images of the ECGE from the top (a, b) and the oblique (c, d) directions. The cathode with a flat surface is covered with CNTs like grass. The roots of CNTs are firmly embedded in the cathode. As shown in Fig. 1(c, d), CNTs are vertically aligned and uniformly distributed in glass substrate, and the vertically aligned CNTs can actively contribute to electron emission when an electric field is applied.

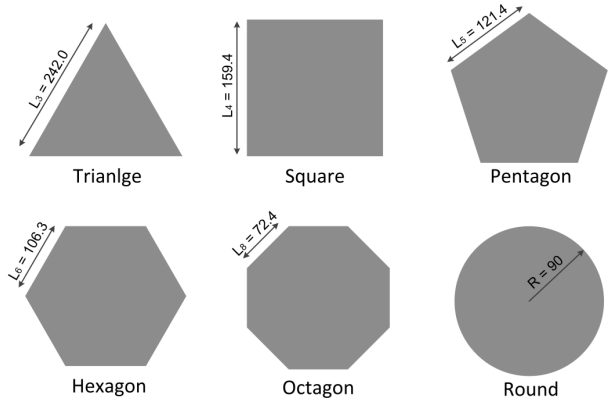


*Figure 2: Field emission cells of different patterns.*

As shown in Fig. 2, models for field emission cells of different shapes were built and investigated by the CST studio. To investigate the edge efforts of different patterns that affected the field emission properties, all of the emitter areas were set as 2.54×10-4 cm2. And the single emission cell was centered at the origin of coordinates (0, 0, 0).

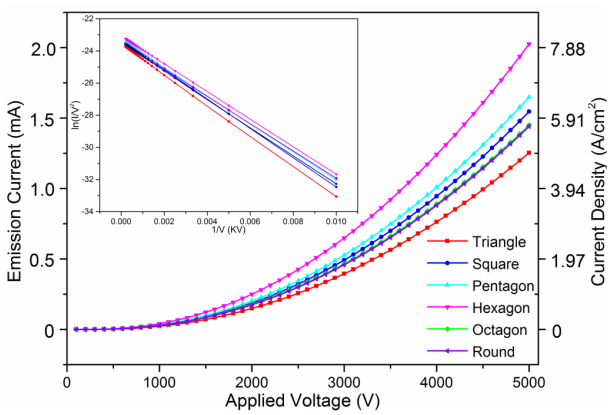


*Figure 3: Field emission properties of different patterns.*

The field emission properties for single emission cells with different patterns were shown in Fig. 3. From those results, we can see that the field emission properties of the cells differ from each other. Applied with the same voltage, the hexagon sample emits the highest current, followed by the pentagon one and the square one. The emission current of the octagon cell is almost the same as the round one. However the triangle one shows poorer emission current. Take applied voltage of 5000 V as an example, the emission current densities for the single triangle, square, pentagon, hexagon, octagon, and round cell are 4.92, 6.10, 6.50, 7.99, 5.71, and 5.67 A/cm2, respectively. From those results above, we can see that, the field emission properties could be affected by changing the patterns.

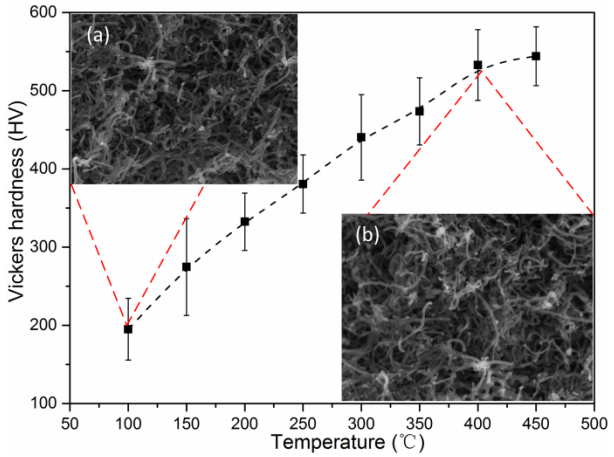


*Figure 4: The relationship between Vickers hardness of the ECGE and the hardening temperature. The insets show the SEMs of (a) the ECGE with hardening procedure of 100 ℃for 4h and (b) the ECGE with hardening procedure of 400 ℃for 4h.*

The relationship between Vickers hardness of the cathode surface and hardening temperature was tested. The Vickers hardness for the samples baked at 100℃ is about 191 HV, and the Vickers hardness for the samples baked at 400℃ is 513 HV. It can be observed in Fig. 4 that the Vickers hardness increased monotonically with the increase of baking temperature. However, the Vickers hardness did not show significant increase beyond 400℃. For the curing process of SG, no change of the Vickers hardness represents that the dehydration process reaches

stable state. The high temperature hardening process performed under 400℃ for 4h could be a preferred procedure for the ECGE fabrication.

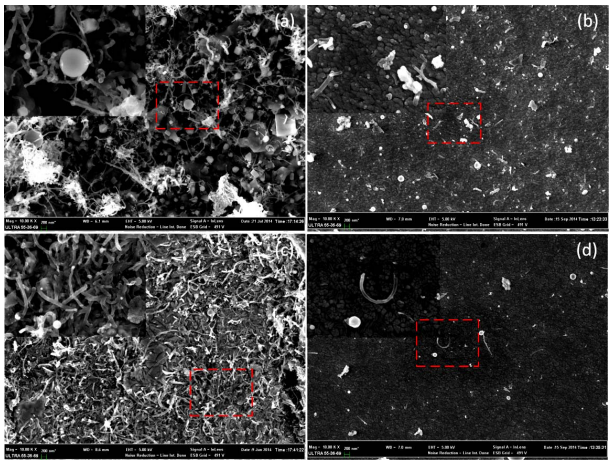


*Figure 5 : SEMs of the ECGE (a) with and (c) without high temperature hardening treatment after field emission; SEM of the opposite anodes of (b) the pristine ECGE and (d) the hardened ECGE.*

Figure 5(a-d) illustrates SEM images of the pristine ECGE and the hardened ECGE with high temperature. The SEM images indicate almost the same surface topography of these two ECGEs before applying strong field. However, their morphologies showed much difference under the action of strong field. For the pristine ECGE, Au spherical particles from the opposite anode with radius of 1~100 nanometers could be observed on the cathode as shown in Fig. 5(a). Accordingly, plenty of CNTs escaped from the cathode and implanted in the anode could be observed on the opposite anode as shown in Fig. 5(b-d) illustrates that Au spherical particles depositing on the cathode and CNTs implanting on the anode significantly reduced.

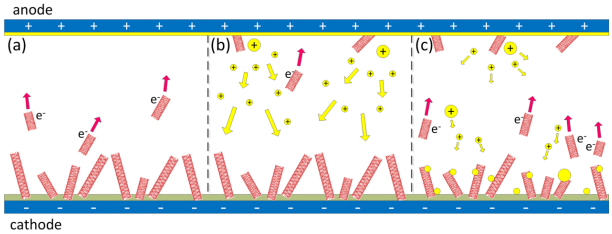


*Figure 6: Schematic diagram for a unstable field emission process of the ECGE.*

Electric field concentration was generated by the electron drift and residual gas ionization on the tip of CNT with tiny curvature radius under strong field. Loosely bonded CNTs easily escaped from the cathode by centralized electrostatic force and then were accelerated in field between the two electrodes (see Fig. 6(a)). They acquired significant energy in this process and flied towards the opposite anode. These CNTs ionized by arcing, which causes their further injuries into the anode surface. The injuring process of the escaping CNTs accompanied with detaching of Au particles with positive electric from the anode surface (see Fig. 6(b)). These Au particles were then accelerated to the cathode with arching and ionization processes. Arcing with high current flow can produce a plasma channel near the cathode surface. CNTs were seriously damaged or sometimes even completely removed from the cathode substrate under action with this plasma channel, which induces more arcing conversely (see Fig. 6(c)). Then the secondary particles would migrate towards the anode where they eject more secondary electrons. The above process would go on repeating and results in contamination on the two electrodes, which is adverse to perform a stable field emission for the ECGE.

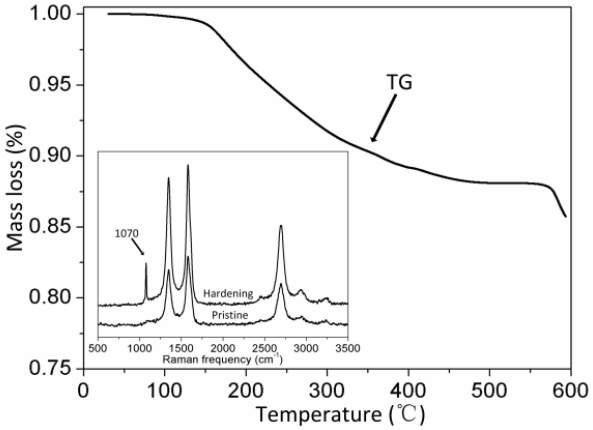


*Figure 7: The thermo-analytical curves TG/DSC of the ECGE film were obtained in air with heating rate of 10℃min-1. The inset shows Raman spectra of the ECGE film before and after the hardening process.*

TG and RS were carried out for the ECGE to understand the strengthening mechanism in high temperature hardening process. TG curve in Fig. 7 shows that the mass loss trend of the ECGE in hardening process. It can be seen in Fig.7 that the weight of the ECGE composited film smoothly decreased from about 130 ℃ to 450 ℃ with heating rate of 10℃/min. The TG curve kept almost steady-state without mass loss till about 550 ℃ after the smooth decreasing process and then sharply decreased. There is about 13% mass loss from 130 ℃ to 450 ℃, which is mainly caused by the loss of absorbed water and crystal water. And the sharp mass loss at 570 ℃ is caused by the combustion of CNT. The bonding layer of SG around CNTs will undergo this dehydration process under high temperature and form a stable adhesive layer. The structural features of these stable adhesive layers were further investigated using RS measurements. As shown in the inset of Fig.8 two RS curves were obtained for the pristine ECGE and the hardened ECGE. Three Raman bonds at 1,580 (G bond), 1,350 (D bond), and 2,650 cm-1 (2D bond) can be observed for the pristine CNTs, which attributes to the Raman-active, in-plane atomic displacement E2g mode, disorder-induced features of the CNTs and the overtone of D bond. In the hardened sample, one more bond at 1070 cm-1 can be observed, which is due to the vibration of -Si-O- bond in silicon dioxide sheet. The -Si-O- film achieved around CNTs by the high temperature hardening treatment improve the bonding strength between SG and CNTs because more bonding positions will be produced at bonding interface for Solid state bonding when water molecules gave ways during dehydration process.

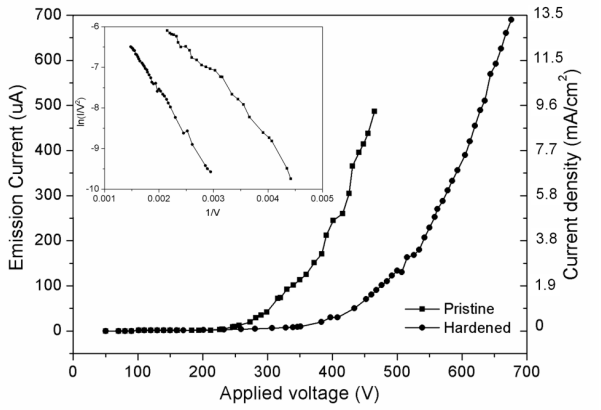


*Figure 8: Emission current vs. electric field curves of the pristine emitter and the hardened emitter. The inset represents the FN plots derived from the curves of current vs. electric fields.*

The field emission characteristics of the field emitter before and after harden process were tested in a vacuum chamber. The relationship of the emission current with the applied voltage is shown in Fig. 8. Both of the emission currents increase monotonically with the applied field. The turn-on field, that defined as an electric field required to get an emission current of 10 μA, were 249 V and 351 V for the pristine and the hardened emitter respectively. We simply consider the total area of the emission cells on the emitter as the emission area. The area $S=51*\pi*(Ø/2)^2 = 0.052\ cm^2$. For the hardened emitter, with the applied voltage of 676 V, the field emission current of 0.69 mA and the current density of 13.27 $mA/cm^2$ was achieved. In Fig. 6, the emission current curve seems to show a "linear" relation with the applied field from 550-700 V. The phenomenon was caused by the current-limiting resistor who shared the voltage of the field emitter in the circuit. The corresponding Fowler-Nordheim (F-N) plot for the flexible emitter is shown in the inset.

## CONCLUSIONS

In summary, we have performed the stress distribution on the cathode using COMSOL. Our simulation revealed that the junction area of the CNT, the cathode surface and the vacuum domain suffers the maximum stress. It indicated that the high bonding strength between the binder and the CNT is crucial for avoiding escaping of the CNTs from the cathode surface under strong field. A dehydration process during hardening treatment provides more adhesion positions for solid state bonding between SG and CNTs. So a reasonable high temperature hardening process is beneficial for the ECGE to obtain more stable adhesive interfacial layer between SG and CNTs. The RS test shows that the firm -Si-O- film formed around the CNTs after the obvious mass loss process, which is detected by TG analysis. SEMs shows that the escaping CNTs from the cathode of the hardened ECGE are greatly reduced compared with the pristine ECGE. The above high temperature hardening process greatly improves the adhesive strength between SG and CNTs. As a result, the field emission property was also significantly enhanced. The turn on field of the ECGE decreased from 1.52 V/um to 0.74 V/um after the hardening treatment. Meanwhile, the better emission stability of 40 hours for 32% degradation of emission current from 344 uA was also achieved. The developed ECGE could be sufficient using as electron source for various field emission devices, including lighting devices and X-ray tubes, yet further optimization is required in device configuration and processing.

## REFERENCES

[1] W. B. Choi, "Fully sealed, high-brightness carbon nanotube field-emission display," Applied Physics Letters, vol. 75, p. 3129, 1999.

[2] S. S. Fan, "Self-oriented regular arrays of carbon nanotubes and their field emission properties," Science, vol. 283, pp. 512-514, Jan 22 1999.

[3] M. Deng, "Fabrication of Ni-matrix carbon nanotube field emitters using composite electroplating and micromachining," Carbon, vol. 47, pp. 3466-3471, Dec 2009.

[4] H. C. Wu , "Fabrication of double-sided field-emission light source using a mixture of carbon nanotubes and phosphor sandwiched between two electrode layers," Carbon, vol. 50, pp. 4781-4786, Nov 2012.

[5] J. S. Park, "X-ray images obtained from cold cathodes using carbon nanotubes coated with gallium-doped zinc oxide thin films," Thin Solid Films, vol. 519, pp. 1743-1748, Dec 30 2010.

[6] S. H. Heo, "Transmission-type microfocus x-ray tube using carbon nanotube field emitters," Applied Physics Letters, vol. 90, Apr 30 2007.

[7] B. Gao, "Fabrication and electron field emission properties of carbon nanotube films by electrophoretic deposition," Advanced Materials, vol. 13, pp. 1770-1773, Dec 2001.

[8] R. Longtin, "High-temperature processable carbon-silicate nanocomposite cold electron cathodes for miniature X-ray sources," Journal of Materials Chemistry C, vol. 1, pp. 1368-1374, 2013.

[9] J. H. Park, "Field emission properties and stability of thermally treated photosensitive carbon nanotube paste with different inorganic binders," Diamond and Related Materials, vol. 14, pp. 2113-2117, Nov-Dec 2005.

[10] J.-H. Park, "Stable and high emission current from carbon nanotube paste with spin on glass," Journal of Vacuum Science & Technology B: Microelectronics and Nanometer Structures, vol. 23, p. 702, 2005.

[11] T. Feng, "Memory emission of printed carbon nanotube cathodes," Applied Physics Letters, vol. 88, May 15 2006.

[12] J. M. Ha, "Highly stable carbon nanotube field emitters on small metal tips against electrical arcing," Nanoscale Research Letters, vol. 8, Aug 16 2013.

[13] J. W. Kim, "Highly reliable field electron emitters produced from reproducible damage-free carbon nanotube composite pastes with optimal inorganic fillers," Nanotechnology, vol. 25, Feb 14 2014.

## CONTACT

*Y. Wang, tel: +86 151-2112-8875; wyyw@sjtu.edu.com